Eur. Phys. J. C (2024) 84:284
https://doi.org/10.1140/epjc/s10052-024-12648-2

THE EUROPEAN PHYSICAL JOURNAL C

Regular Article - Theoretical Physics

Black hole in discrete gravity

Ali H. Chamseddine[1], **Ola Malaeb**[1,2,a], **Sara Najem**[1,2]

[1] Department of Physics, American University of Beirut, Beirut, Lebanon
[2] Center for Advanced Mathematical Sciences, American University of Beirut, Beirut, Lebanon

Received: 8 November 2023 / Accepted: 6 March 2024

Abstract We study the metric corresponding to a three-dimensional coset space $SO(4)/SO(3)$ in the lattice setting. With the use of three integers n_1, n_2, and n_3, and a length scale, l_μ, the continuous metric is transformed into a discrete space. The numerical outcomes are compared with the continuous ones. The singularity of the black hole is explored and different domains are studied.

1 Introduction

The challenges encountered while attempting to quantize gravity have inspired the advancement of discrete gravity theories. Different approaches to lattice gravity were explored over the past years [1,8,11]. Lately, in [6], a new approach to discrete gravity was proposed where the manifold is taken to be discrete and consists of elementary cells. The dimension d is defined assuming each cell has $2d$ neighboring cells that share a common boundary with each individual cell, and a finite number of degrees of freedom is associated with each cell. This approach stands out from others primarily because it clearly reveals the continuous limit.

Recently and based on the above model, the scalar curvature of discrete gravity in two dimensions was investigated in [4], while the examination of the curvature tensor in three dimensions can be found in [5]. In the latter, a three-sphere was considered and its continuous metric was converted into a lattice. It was shown that the scalar curvature in the discrete space approaches the expected value in the continuous limit.

In this paper, we will study again the three-dimensional case, but now for a black hole coset space metric. To discretize, a length scale l_μ and three integers n_1, n_2, n_3 are used. The metric corresponding to a three-dimensional coset space, along with the spin connections and curvatures in the continuous case, are presented in the Sect. 2. In Sect. 3, we discretize the continuous metric of the black hole coset space. We investigate the domains in the proximity of the singularities and away from them, and numerically compare the discrete values of the curvature tensor with the expected continuous ones.

2 Black hole coset space metric

Consider the metric corresponding to a three-dimensional coset space $SO(4)/SO(3)$ [3,7]

$$ds^2 = \frac{\tanh^2 z}{u}dx^2 + \frac{\coth^2 z}{u}dy^2 + dz^2, \tag{1}$$

where

$$u = 1 - \left(x^2 + y^2\right), \quad u \geq 0, \quad -\infty \leq z \leq \infty. \tag{2}$$

A coset space of the form G/H is the space of elements where $g \in G$ can be decomposed in the form:

$$g = kh \in G, \quad k = \exp\left(i\theta^{i4}J_{i4}\right) \in G/H,$$
$$h = \exp\left(i\theta^{ij}J_{ij}\right), \quad i, j = 1, 2, 3.$$

This metric was first obtained to represent a configuration of a metric in the presence of a dilation field, but we will not add a dilation here. This choice is of particular interest because the lattice is not trivial and not maximally symmetric. The z-behaviour is different than the x and y. Upon letting

$$\theta^1 = \frac{\tanh z}{\sqrt{u}}dx, \quad \theta^2 = \frac{\coth z}{\sqrt{u}}dy, \quad \theta^3 = dz$$

be the three one-forms, the spin connections and curvature tensors are all computed. The scalar curvature is then given by

$$R = -4\left(1 + \frac{1}{\sinh^2 z \cosh^2 z} + \frac{1}{u}\left(y^2 \tanh^2 z + x^2 \coth^2 z\right)\right). \tag{3}$$

[a] e-mail: oh09@aub.edu.lb (corresponding author)

Published online: 19 March 2024

Since $u \geq 0$, R will always have negative curvature. There is a singularity at all points on the circle defined by $u = 0$ and at $z = 0$. We can further confirm this by calculating the curvature invariant $R^{ab}R_{ab}$

$$R^{ab}R_{ab} = (R_{11})^2 + (R_{22})^2 + (R_{33})^2 + 2(R_{12})^2 + 2(R_{13})^2 + 2(R_{23})^2 .$$

It is worth noting that the coordinate system we are using cannot be extended. It is an Euclidean black hole with no horizon. The singularities are for $z = 0$ and on the boundary of the disc with $x^2 + y^2 = 1$, i.e. $u = 0$.

To relate it to the lattice setting, the metric used here gives the curvature tensor in flat coordinates (anholonomic system). This is the system where:

$$\theta^1 = e^1_{\dot{1}}dx, \quad \theta^2 = e^2_{\dot{2}}dy, \quad \theta^3 = e^3_{\dot{3}}dz$$

so that:

$$e^1_{\dot{1}} = \frac{\tanh z}{\sqrt{u}}, \quad e^2_{\dot{2}} = \frac{\coth z}{\sqrt{u}}, \quad e^3_{\dot{3}} = 1. \tag{4}$$

Thus, we will have:

$$R_{\mu\nu}{}^{ij} = e^k_\mu e^l_\nu R_{kl}{}^{ij}.$$

In terms of components, we will have:

$$R_{\dot{1}\dot{2}}{}^{ij} = e^1_{\dot{1}}e^2_{\dot{2}}R_{12}{}^{ij}, \quad R_{\dot{1}\dot{3}}{}^{ij} = e^1_{\dot{1}}e^3_{\dot{3}}R_{13}{}^{ij},$$
$$R_{\dot{2}\dot{3}}{}^{ij} = e^2_{\dot{2}}e^3_{\dot{3}}R_{23}{}^{ij}.$$

For the non-vanishing components, we have

$$R_{\dot{1}\dot{3}}{}^{13} = \frac{2\sinh z}{\sqrt{u}\cosh^3 z}, \quad R_{\dot{1}\dot{2}}{}^{13} = -\frac{2y}{u^{\frac{3}{2}}\cosh^2 z},$$
$$R_{\dot{2}\dot{3}}{}^{23} = -\frac{2\cosh z}{\sqrt{u}\sinh^3 z}, \quad R_{\dot{1}\dot{2}}{}^{23} = -\frac{2x}{u^{\frac{3}{2}}\sinh^2 z},$$
$$R_{\dot{1}\dot{3}}{}^{12} = -\frac{2y\sinh z}{u\cosh^3 z}, \quad R_{\dot{2}\dot{3}}{}^{12} = -\frac{2x\cosh z}{u\sinh^3 z},$$
$$R_{\dot{1}\dot{2}}{}^{12} = -\frac{2}{u}\left(1 + \frac{1}{u}\left(y^2\tan^2 z + x^2\cot^2 z\right)\right).$$

We note that we can compare with the discrete case by observing that:

$$R_{\dot{1}\dot{3}}{}^{13} = -R_{\dot{1}\dot{3}}{}^{2}, \quad R_{\dot{1}\dot{2}}{}^{13} = -R_{\dot{1}\dot{2}}{}^{2},$$
$$R_{\dot{2}\dot{3}}{}^{23} = R_{\dot{2}\dot{3}}{}^{1}, \quad R_{\dot{1}\dot{2}}{}^{23} = R_{\dot{1}\dot{2}}{}^{1},$$
$$R_{\dot{1}\dot{3}}{}^{12} = R_{\dot{1}\dot{3}}{}^{3}, \quad R_{\dot{2}\dot{3}}{}^{12} = R_{\dot{2}\dot{3}}{}^{3}, \quad R_{\dot{1}\dot{2}}{}^{12} = R_{\dot{1}\dot{2}}{}^{3}.$$

3 Discretizition and numerics

In order to discretize, we follow the same methodology we used in [5]. Explicitly, we define:

$$\ell_1 = \ell_2 = \ell_3 = \frac{1}{N}, \quad x = \frac{n_1}{N}, \quad y = \frac{n_2}{N}, \quad z = \frac{n_3}{N}, \tag{5}$$

where

$$n_1 = 1, 2, \ldots N, \quad n_2 = 1, 2, \ldots N, \quad n_3 = 1, 2, \ldots N, \tag{6}$$

which together with the constraint (from Eq. 2) give:

$$u = 1 - \frac{n_1^2 + n_2^2}{N^2} > 0. \tag{7}$$

Discretization is required in all three dimensions, x, y, and z; therefore, in terms of numerical complexity, the code is $\mathcal{O}(N^3)$. Hence, expanding the lattice would scale as N^3.

To derive the three-dimensional discrete curvature, we start with the definition [6]

$$\begin{aligned}
\frac{i}{2}R^i_{\mu\nu}\sigma^i &= \frac{1}{2\ell^\mu\ell^\nu}\Big(\Omega_\mu(n)\,\Omega_\nu(n+\widehat{\mu})\,\Omega_\mu^{-1}(n+\widehat{\nu}) \\
&\quad \Omega_\nu^{-1}(n) - \mu \leftrightarrow \nu\Big) \\
&= \frac{1}{2\ell^\mu\ell^\nu}\Big\{\Big(\cos\frac{1}{2}\ell^\mu\omega_\mu(n) + i\widehat{\omega}^i_\mu(n) \\
&\quad \sin\frac{1}{2}\ell^\mu\omega_\mu(n)\,\sigma^i\Big) \\
&\quad \cdot\Big(\cos\frac{1}{2}\ell^\nu\omega_\nu(n+\widehat{\mu}) + i\widehat{\omega}^i_\nu \\
&\quad (n)\sin\frac{1}{2}\ell^\nu\omega_\nu(n+\widehat{\mu})\,\sigma^i\Big) \\
&\quad \cdot\Big(\cos\frac{1}{2}\ell^\mu\omega_\mu(n+\widehat{\nu}) - i\widehat{\omega}^i_\mu(n+\widehat{\nu}) \\
&\quad \sin\frac{1}{2}\ell^\mu\omega_\mu(n+\widehat{\nu})\,\sigma^i\Big) \\
&\quad \cdot\Big(\cos\frac{1}{2}\ell^\nu\omega_\nu(n) - i\widehat{\omega}^i_\nu(n)\sin\frac{1}{2}\ell^\nu \\
&\quad \omega_\nu(n)\,\sigma^i\Big) - \mu \leftrightarrow \nu\Big\}.
\end{aligned}$$

Consider the product

$$\Big(\cos\frac{1}{2}\ell^\mu\omega_\mu(n) + i\widehat{\omega}^i_\mu(n)\sin\frac{1}{2}\ell^\mu\omega_\mu(n)\,\sigma^i\Big)$$
$$\Big(\cos\frac{1}{2}\ell^\nu\omega_\nu(n+\widehat{\mu}) + i\widehat{\omega}^i_\nu(n+\widehat{\mu})\sin\frac{1}{2}\ell^\nu\omega_\nu(n+\widehat{\mu})\,\sigma^i\Big),$$

this can be rewritten as:

$$\begin{aligned}&\left(\cos\frac{1}{2}\ell^{\mu}\omega_{\mu}(n)\cos\frac{1}{2}\ell^{\nu}\omega_{\nu}(n+\widehat{\mu})-\widehat{\omega}_{\mu}^{i}(n)\widehat{\omega}_{\nu}^{i}(n+\widehat{\mu})\right.\\&\quad\left.\sin\frac{1}{2}\ell^{\mu}\omega_{\mu}(n)\sin\frac{1}{2}\ell^{\nu}\omega_{\nu}(n+\widehat{\mu})\right)\\&\quad+i\left(\cos\frac{1}{2}\ell^{\mu}\omega_{\mu}(n)\widehat{\omega}_{\nu}^{i}(n+\widehat{\mu})\sin\frac{1}{2}\ell^{\nu}\omega_{\nu}(n+\widehat{\mu})\right.\\&\quad+\widehat{\omega}_{\mu}^{i}(n)\sin\frac{1}{2}\ell^{\mu}\omega_{\mu}(n)\cos\frac{1}{2}\ell^{\nu}\omega_{\nu}(n+\widehat{\mu})\\&\quad\left.\epsilon^{ijk}\widehat{\omega}_{\mu}^{j}(n)\sin\frac{1}{2}\ell^{\mu}\omega_{\mu}(n)\widehat{\omega}_{\nu}^{k}(n+\widehat{\mu})\sin\frac{1}{2}\ell^{\nu}\omega_{\nu}(n+\widehat{\mu})\right)\sigma^{i}\\&\equiv A_{\nu\mu}+iB_{\mu\nu}^{i}\sigma^{i},\end{aligned}$$

where

$$\begin{aligned}A_{\mu\nu}(n)=&\left(\cos\frac{1}{2}\ell^{\mu}\omega_{\mu}(n+\widehat{\nu})\cos\frac{1}{2}\ell^{\nu}\omega_{\nu}(n)-\widehat{\omega}_{\mu}^{j}(n+\widehat{\nu})\widehat{\omega}_{\nu}^{j}(n)\right.\\&\left.\sin\frac{1}{2}\ell^{\mu}\omega_{\mu}(n+\widehat{\nu})\sin\frac{1}{2}\ell^{\nu}\omega_{\nu}(n)\right),\end{aligned}$$

and:

$$\begin{aligned}B_{\mu\nu}^{i}(n)=&\left(\widehat{\omega}_{\mu}^{i}(n)\sin\frac{1}{2}\ell^{\mu}\omega_{\mu}(n)\cos\frac{1}{2}\ell^{\nu}\omega_{\nu}(n+\widehat{\mu})\right.\\&+\widehat{\omega}_{\nu}^{i}(n+\widehat{\mu})\\&\sin\frac{1}{2}\ell^{\nu}\omega_{\nu}(n+\widehat{\mu})\cos\frac{1}{2}\ell^{\mu}\omega_{\mu}(n)-\epsilon^{ijk}\widehat{\omega}_{\mu}^{j}(n)\\&\left.\sin\frac{1}{2}\ell^{\mu}\omega_{\mu}(n)\widehat{\omega}_{\nu}^{k}(n+\widehat{\mu})\sin\frac{1}{2}\ell^{\nu}\omega_{\nu}(n+\widehat{\mu})\right).\end{aligned}$$

Similarly, the next pair gives

$$\begin{aligned}&\left(\cos\frac{1}{2}\ell^{\mu}\omega_{\mu}(n+\widehat{\nu})-i\widehat{\omega}_{\mu}^{i}(n+\widehat{\nu})\sin\frac{1}{2}\ell^{\mu}\omega_{\mu}(n+\widehat{\nu})\sigma^{i}\right)\\&\quad\left(\cos\frac{1}{2}\ell^{\nu}\omega_{\nu}(n)-i\widehat{\omega}_{\nu}^{i}(n)\sin\frac{1}{2}\ell^{\nu}\omega_{\nu}(n)\sigma^{i}\right)\\&=A_{\mu\nu}(n)-iB_{\nu\mu}^{i}(n).\end{aligned}$$

Thus, the total product is

$$\begin{aligned}\frac{i}{2}R_{\mu\nu}^{i}\sigma^{i}=&\left(\frac{1}{2\ell^{\mu}\ell^{\nu}}\left(A_{\nu\mu}+iB_{\mu\nu}^{i}\sigma^{i}\right)\left(A_{\mu\nu}-iB_{\nu\mu}^{i}\sigma^{i}\right)\right.\\&\left.-\mu\leftrightarrow\nu\right)\\=&\frac{i}{\ell^{\mu}\ell^{\nu}}\left(A_{\mu\nu}B_{\mu\nu}^{i}-A_{\nu\mu}B_{\nu\mu}^{i}+i\epsilon^{ijk}B_{\mu\nu}^{j}B_{\nu\mu}^{k}\right)\sigma^{i},\end{aligned}$$

giving the below result

$$\begin{aligned}R_{\mu\nu}^{i}(n)=&\frac{2}{\ell^{\mu}\ell^{\nu}}\left(A_{\mu\nu}(n)B_{\mu\nu}^{i}(n)-A_{\nu\mu}(n)B_{\nu\mu}^{i}(n)\right.\\&\left.+\epsilon^{ijk}B_{\mu\nu}^{j}(n)B_{\nu\mu}^{k}(n)\right).\end{aligned}\tag{8}$$

The connection $\omega_{\nu}(n)$ is determined from the zero torsion condition, which is given by

$$\begin{aligned}T_{\mu\nu}(n)=&\frac{1}{\ell^{\mu}}\left(\Omega_{\mu}(n)e_{\nu}(n+\widehat{\mu})\Omega_{\mu}^{-1}(n)-e_{\nu}(n)\right)\\&-\mu\leftrightarrow\nu,\end{aligned}\tag{9}$$

where this equation is written in a contracted form where the vielbeins e_{α}^{a} are incorporated into the Clifford algebra. Upon computing this, we get

$$\begin{aligned}0=&\frac{1}{\ell^{\mu}}\left(\left(\cos\frac{1}{2}\ell^{\mu}\omega_{\mu}(n)+i\widehat{\omega}_{\mu}^{i}(n)\sin\frac{1}{2}\ell^{\mu}\omega_{\mu}(n)\sigma^{i}\right)\sigma^{k}\right.\\&\left(\cos\frac{1}{2}\ell^{\mu}\omega_{\mu}(n)-i\widehat{\omega}_{\mu}^{j}(n)\sin\frac{1}{2}\ell^{\mu}\omega_{\mu}(n)\sigma^{j}\right)e_{\nu}^{k}(n+\widehat{\mu})\\&\left.-e_{\nu}^{i}(n)\sigma^{i}\right)-\mu\leftrightarrow\nu).\end{aligned}$$

By expanding and grouping terms, we get the following result:

$$\begin{aligned}T_{\mu\nu}{}^{i}(n)=&\frac{1}{\ell^{\mu}}\left(\cos\ell^{\mu}\omega_{\mu}(n)e_{\nu}^{i}(n+\widehat{\mu})-\epsilon^{ijk}\right.\\&\sin\ell^{\mu}\omega_{\mu}(n)\widehat{\omega}_{\mu}^{j}(n)e_{\nu}^{k}(n+\widehat{\mu})+2\widehat{\omega}_{\mu}^{i}(n)\\&\left.\widehat{\omega}_{\mu}^{j}(n)\sin^{2}\frac{1}{2}\ell^{\mu}\omega_{\mu}(n)e_{\nu}^{j}(n+\widehat{\mu})-e_{\nu}^{i}(n)\right)\\&-(\mu\leftrightarrow\nu).\end{aligned}$$

The vanishing of $T_{\mu\nu}{}^{i}$ provides 9 conditions to solve for the 9 unknowns $\omega_{\mu}^{i}(n)$. The values of the spin connections are obtained numerically, and hence, the three-dimensional discrete curvatures are obtained using Eq. (8).

Equation 3 gives the expression of the scalar curvature in the continuous case. We are going to compare it with what we get from the discrete case. In the latter, the expression of the scalar curvature is given by:

$$R=2\left(\frac{1}{e_{1}^{1}e_{2}^{2}}R_{12}^{3}+\frac{1}{e_{2}^{2}e_{3}^{3}}R_{23}^{1}+\frac{1}{e_{3}^{3}e_{1}^{1}}R_{31}^{2}\right),$$

which holds when e_{μ}^{i} is diagonal, which is the case here as it is evident from Eq. 4. It is clear from (3) that there is a singularity at $z=0$ and at all points on the circle defined by $u=0$. First, we will examine the domain where z is large, followed by an analysis of the domain where z is small.

3.1 The limit of large z

$$R\to-\frac{4}{u}\left(1+\frac{x^{2}+y^{2}}{u}\right).\tag{10}$$

The singularity at $u=0$ is evident. Therefore, in order to determine the permissible range over which the curvature is

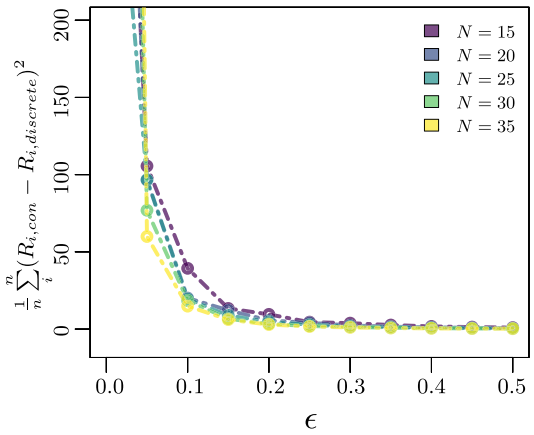

Fig. 1 The rms error between the continuous and discrete values of the scalar curvature in the limit of large z are plotted as a function of ϵ for different N, where ϵ denotes the distance away from $u = 0$ where the discretization is expected to hold. We note that the approach to $\epsilon = 0$ where the locus of the singularity leads to a blow-up in the RMS

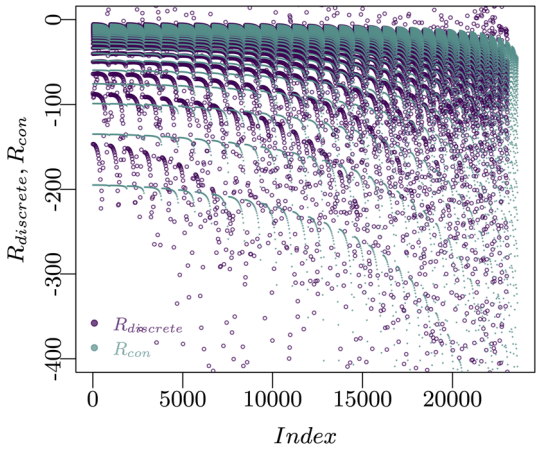

Fig. 2 R continuous and discrete for $N = 35$ and $\epsilon = 0.15$

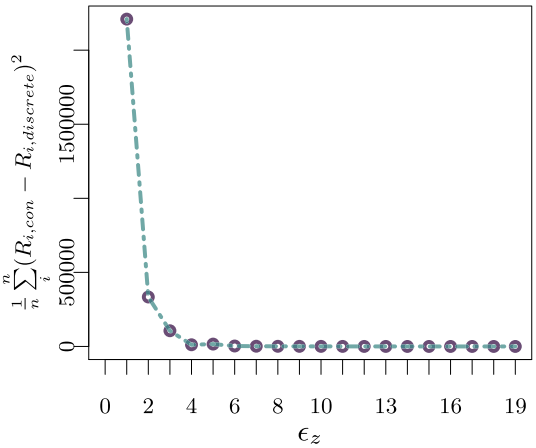

Fig. 3 The RMS error is followed as a function of ϵ_z for $N = 35$ and $\epsilon = 0.15$

well-behaved, we define $1 - x^2 - y^2 > \epsilon$, the range of coordinates in the vicinity of the singularity. We note that $\epsilon = 0$ is the locus of $u = 0$ or equivalently $x^2 + y^2 = 1$, and thus finding the right value of ϵ is equivalent to finding the proper cut-off to avoid the singularity. Therefore, we iterate over different values of ϵ between 0 and 0.5 in increments of 0.05, and calculate the mean-square error between the continuous value of the scalar curvature and its discrete numerical counterpart defined to be $\frac{1}{n}\sum_i^n (R_{i,con} - R_{i,numerical})^2$. We repeat the process for different values of N. The results are plotted in Fig. 1. The different colors correspond to different values of N. We conclude from the plot that the error is converging to zero for $\epsilon = 0.15$.

For ϵ smaller than 0.15, we are close to the singularity ($u = 0$) and the discretization method fails to agree with the continuous limit as the RMS error between R_{con} and $R_{discrete}$ blows up. In the limit where they are in agreement, we show a sample in Fig. 2 for $N = 35$ and $\epsilon = 0.15$, where we plot the values of R_{con} and those of $R_{discrete}$ on the same graph with the index i denoting the element number in the curvature vector associated with given coordinates x_i, y_i and z_i.

3.2 The limit of small z

For a small value of z, we are in the region near the singularity $z = 0$. Therefore, and following the same reasoning we did to find ϵ near $u = 0$, we limit z between ϵ_z/N and 1 and follow the RMS between the continuous and discrete values of the scalar curvature. In Fig. 3, we show the RMS for $N = 35$ and $\epsilon = 0.15$, which allows us to define the lower cutoff near $z = 0$ below which the scalar curvature will blow up.

It is evident from the plot that as ϵ_z approaches 5, the error tends to zero. Further, in order to show the well-behavedness of the discrete scalar curvature, we follow it together with its continuous counterpart in this domain. Figure 4 shows the finiteness of $R_{discrete}$ as opposed to the large, near-singular behavior of R_{con}. The inset shows their agreement away from the jumps.

For very small z, we have $\sinh z \to z$ and $\cosh z \to 1$,

$$R \to -4\left(1 + \frac{1}{z^2} + \frac{1}{u}\left(y^2 z^2 + \frac{x^2}{z^2}\right)\right) \tag{11}$$

$$\simeq -4\left(\frac{1 - y^2}{uz^2}\right) \tag{12}$$

with obvious asymmetry. Figure 5 is obtained by plotting $R_{discrete}$ and $R_{limit} = -4\left(\frac{1-y^2}{uz^2}\right)$ for small values of z, showing their agreement.

Further, when $x = 0$ we get $R \to -4N^2$, displaying clearly the singularity of the black hole. In Fig. 6, the discrete value of the scalar curvature is plotted for $z \simeq \frac{1}{N}$ and $x = 0$ along with its expected limiting behavior, which is $-4N^2$.

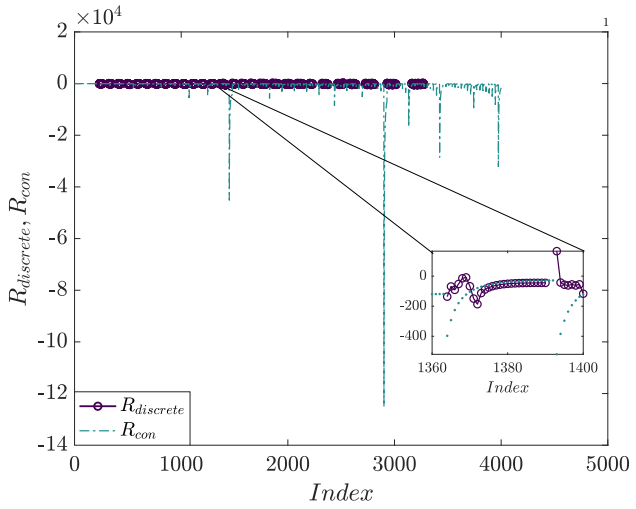

Fig. 4 R continuous and discrete are followed for $N = 35$, $\epsilon = 0.15$, $z < 1$, and $\epsilon_z = 5$. The inset shows their local agreement and makes it obvious that R_{con} exhibits large near-singular jumps, which are avoided in the discrete case

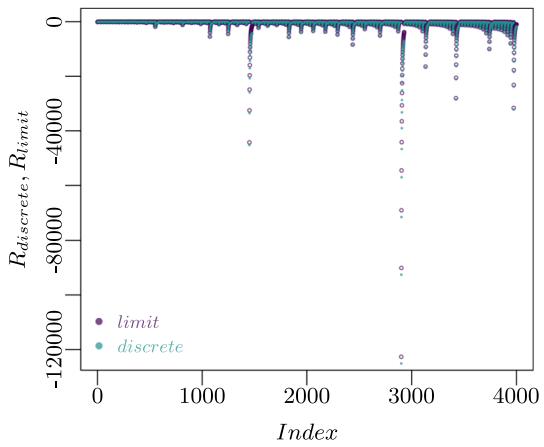

Fig. 5 $R_{discrete}$ is compared with its limiting behavior $4(\frac{1-y^2}{uz^2})$ for small z

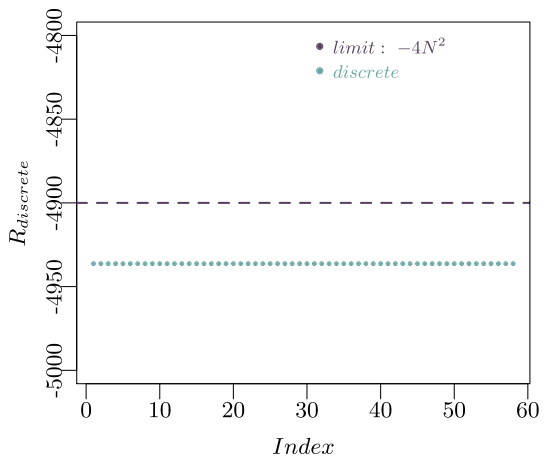

Fig. 6 $R_{discrete}$ is compared with its limiting value $-4N^2$ for $z \approx \frac{1}{N}$ and $x = 0$

4 Conclusion

In this paper, we applied the methodology used in [5] to define the curvature of the discrete space in the proposed model of discrete gravity. We considered the black hole coset space metric. The singularities were studied, and the curvatures in the discrete and continuous limits were compared close and far away from the singularity. We found that as we move away from the singularity, the rms error between the two curvatures tends to zero. We also showed that near the singularity, the discrete method is more reliable than the continuous.

Our contribution to the literature on black holes and numerical relativity is that it introduces a discrete approach complementing the prevailing continuum counterpart. This sets the ground for the calculations of curvatures for arbitrary surfaces. Further, the introduction of our method in the context of naked singularities establishes a mathematical and numerical framework to be generalized to $4D$. Unlike the general concern of numerical relativity in answering questions about dynamics around black holes and their properties [2,9,10,12], our work is an experimentation on the limitation of discrete gravity and its accompanying numerics and whether it is generalizable to $4D$. The next step is to address how to calculate the metric and curvature of an arbitrary closed surface.

Acknowledgements The work of A. H. C. is supported in part by the National Science Foundation Grant No. Phys-2207663.

Data availability This manuscript has no associated data or the data will not be deposited. [Authors' comment: This is a theoretical study and no experimental data.]

Code availability This manuscript has associated code/software in a data repository. [Authors' comment: This manuscript has associated code in a data repository. The script used in the paper is available at the following link: https://www.dropbox.com/scl/fo/gtpfyi67r4n9vh5pme3ea/h?rlkey=ihlonza5yuldapie06qoc01y0&dl=0.]

Funded by SCOAP[3].

References

1. S. Catterall, J. Kogut, R. Renken, Phase structure of four dimensional simplicial quantum gravity. Phys. Lett. B **328**(3–4), 277–283 (1994)
2. S.A. Caveny, M. Anderson, R.A. Matzner, Tracking black holes in numerical relativity. Phys. Rev. D **68**(10), 104009 (2003)
3. A.H. Chamseddine, Asymmetric non-abelian wzw actions and a 3d string model. Phys. Lett. B **275**(1–2), 63–69 (1992)
4. H.A. Chamseddine, O. Malaeb, S. Najem, Scalar curvature in discrete gravity. Eur. Phys. J. C **82**(7), 651 (2022)
5. A.H. Chamseddine, O. Malaeb, S. Najem, Curvature tensor in discrete gravity. Eur. Phys. J. C **83**, 896 (2023)
6. A.H. Chamseddine, V. Mukhanov, Discrete gravity. J. High Energy Phys. **2021**(11), 1–13 (2021)
7. E.S. Fradkin, V.Y. Linetsky, On space-time interpretation of the coset models in d< 26 critical string theory. Phys. Lett. B **277**(1–2), 73–78 (1992)
8. T. Regge, General relativity without coordinates. Il Nuovo Cimento **1955–1965**(19), 558–571 (1961)
9. R. Shaikh, P. Kocherlakota, R. Narayan, P.S. Joshi, Shadows of spherically symmetric black holes and naked singularities. Mon. Not. R. Astron. Soc. **482**(1), 52–64 (2019)
10. M. Shibata, M. Sasaki, Black hole formation in the Friedmann universe: formulation and computation in numerical relativity. Phys. Rev. D **60**(8), 084002 (1999)
11. K.G. Wilson, Confinement of quarks. Phys. Rev. D **10**(8), 2445 (1974)
12. M. Zhang, J. Jiang, Curvature induced scalarization of Kerr–Newman black hole spacetimes. Phys. Rev. D **107**(4), 044002 (2023)